water

MDPI

Review

Quantification of Groundwater Hazards Related to Fluvial Floods via Groundwater Flow Modelling: A Review

Jaromír Říha , Tomáš Julínek * and David Duchan

Institute of Water Structures, Faculty of Civil Engineering, Brno University of Technology, 602 00 Brno, Czech Republic
* Correspondence: julinek.t@vutbr.cz

Abstract: Flood-related issues include the impact of groundwater on flood protection measures and other subsurface structures in a protected area. At the same time, subsurface elements of flood protection structures may significantly influence the natural groundwater regime and affect existing structures during non-flood periods. The paper provides an overview of hazardous factors linked to groundwater and specifies variables for the quantification of related hazards. Appropriate hydraulic groundwater flow models are presented and discussed, and their suitability for the modelling of individual typical problems and for hazard quantification is specified. The use of models and the application of CAD and GIS tools for data pre- and post-processing is mentioned in brief and demonstrated on examples of typical practical situations.

Keywords: modelling; groundwater; flood protection; groundwater flooding; groundwater hazards

1. Introduction

Increased water stages during flood events can significantly affect the regime of groundwater flow in aquifers adjacent to rivers. The rise of the water level in a watercourse during a flood results in temporary infiltration along the banks of the river and seepage propagation into the aquifer in the opposite direction to that of normal flow. The piezometric level rises and may cause what has been termed a "groundwater flood" [1,2], which may endanger both flood protection elements and subsurface parts of structures in protected urbanized areas [3–5]. This effect may result in the waterlogging of terrain behind flood protection barriers [6–8].

During the last decades, several extreme floods took place in Central Europe. In March and April of 2006, floods occurred due to long-term precipitation combined with snow melting. In July 1997, August 2002, and June 2013, floods took place as a result of persistent rainfall in large areas [9,10]. During these events, groundwater flooding happened at most of the affected localities protected by the flood protection systems. For example, in the village of Troubky, a significant difference between the water level in the river and the terrain behind the FPM caused waterlogging of the entire village area. On the contrary, permanent waterlogging occurred in Prague-Zbraslav due to the construction of the FPM with deep subsurface parts that blocked the natural drainage to the Vltava River.

In the case of the construction of flood control works, their subsurface parts may also affect the natural groundwater regime during non-flood periods, during which groundwater moves from higher locations towards streams which drain adjacent aquifers [11]. Here, maintaining free communication between the river and aquifer is essential for, inter alia, maintaining base flow in streams [12–14]. Therefore, seepage barriers such as cut-off walls and grout curtains should be designed to be partially penetrable.

Factors such as geological composition (including anthropogenic layers), the historical development of towns in flood plains, river regulation (including flood protection structures), quay walls, the drainage of groundwater into sewerage, etc., have to be taken into

Citation: Říha, J.; Julínek, T.; Duchan, D. Quantification of Groundwater Hazards Related to Fluvial Floods via Groundwater Flow Modelling: A Review. *Water* **2023**, *15*, 1145. https://doi.org/10.3390/w15061145

Academic Editor: Ryan Bailey

Received: 17 February 2023
Revised: 7 March 2023
Accepted: 11 March 2023
Published: 15 March 2023

account when assessing groundwater effects and related hazards. Practically all of the mentioned factors may be implemented into powerful groundwater flow models. Current mathematical modelling methods [15] and existing software enable users to assess the impact of flood protection measures and their subsurface elements on the foundations of flood protection structures and buildings in protected areas under a natural regime, as well as during flood events. Hydraulic calculations allow the evaluation and quantification of flood hazards and their representation using powerful computer graphics softwares.

When evaluating the risks associated with groundwater effects, the vulnerability of affected structures must be taken into account and compared with corresponding hazards. The potential damages and losses must be estimated as well. Although groundwater flooding usually does not result in losses of human life or health, it may cause significant material losses. Finally, the probability of incident must be incorporated into the risk analysis. The proper design of subsurface parts of flood protection barriers may significantly reduce groundwater induced hazard and risk.

The rate of seepage propagation depends on aquifer parameters such as storativity, transmissivity, porosity, saturation of the soil, etc., which should be determined by inverse modelling techniques [16–19]. The "calibration process" depends on simulation conditions (steady-state or transient) and the aquifer type (confined or unconfined). Numerous approaches have been applied, such as particle swarm optimization [20], genetic algorithms or differential evolution [17], nonlinear regression [21], or clonal selection algorithms [22].

For the interpretation of input data and modelling results, mapping techniques based on GIS tools, applications, and databases on water resources (including groundwater issues) have been applied [23]. Even if remote-sensing and GIS techniques have experienced rapid development in recent decades [24–28], their applications for detailed analysis in the areas behind flood protection measures are very limited. Identical tools are also available for web-based solutions of groundwater flow, and the analysis of groundwater sources and pollution risk [23,29–31]. Cloud-based decision support systems have been presented by Jones et al. [32] based on recent and historic water data, including interactive mapping capabilities. A numerical model of groundwater flow and the transport of matter completely integrated in a web environment was described by Glass et al. [33].

Unlike fluvial river flooding and surface water flooding, groundwater flood risk maps are not commonly available to the public. Groundwater risk mapping frameworks are however presented, e.g., by Collins et al. [34] or Merchán-Rivera [35]. Hazard maps for uplift due to rising groundwater during floods have been presented by Julínek et al. [36].

Most of the available studies deal with particular groundwater-related issues, such as groundwater flooding [1,37] or combined modelling involving fluvial flooding interaction with groundwater flow [34,38–42], hazards in karstic lowlands [43], and others, while there is a lack of more comprehensive summaries of groundwater effects in relation to floods and flood protection measures (FPM). This paper provides a list of hazardous factors related to the groundwater regime during flood events, specifies variables for hazard quantification, and proposes appropriate modelling techniques. Individual typical cases are demonstrated for localities in the Czech Republic based on about 50 case studies carried out in the region. The authors thus contribute to the risk analysis of groundwater related issues during the flood and no-flood periods, providing classification and quantification methods for hazard determination. The link between groundwater flow modelling and related hazards is determined as well.

2. Methods

2.1. Rationale

The groundwater problems related to fluvial floods and flood protection measures are quite complex. In Figure 1, a diagram of groundwater flow during a fluvial (river) flood is shown for a situation without (A) and with (B) flood protection measures such as levees or floodwalls. It can be seen that in the case of no FPM with water inundation, the pore pressure in the aquifer is compensated by the weight of overbanked flood water. After installing FPM, the pressure in the aquifer that usually acts on the bed of the relatively impervious topsoil layer may exceed its weight, which may cause uplift failure of the topsoil behind the flood protection arrangements [36]. Such an impact can result in a hazard both to protective elements and to the subsurface parts of structures (e.g., cellars, subsurface garages, etc.) in the protected territory. The threat is posed by the rise of the piezometric head in the aquifer, by the water pressure on the underground parts of civil structures, and by the seepage below the FPM, which via increased hydraulic gradients, may cause internal erosion of the soil close to the foundations of flood protection structures [44]. Seepage into the protected area is also unfavourable during a flood; it increases the amount of "inner water" that must be pumped back into the stream (groundwater flooding). When dealing with hazards related to groundwater effects during the floods, in context with climate changes, one must consider an expected higher intensity of fluvial floods, i.e., higher peak discharges and flood durations [45].

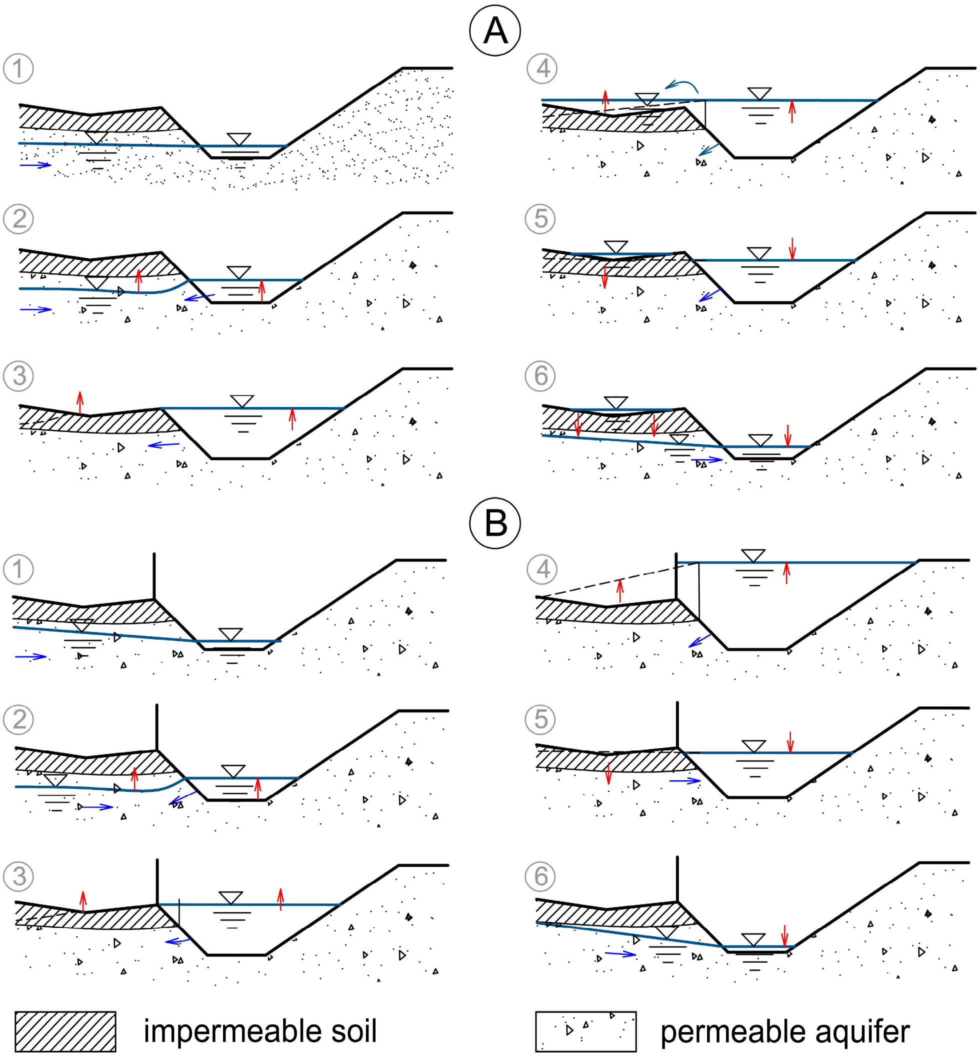

Figure 1. Groundwater flow during a flood. (**A**) no flood protection, (**B**) flood protection. Blue arrows represent water flow direction, red arrows change of water table/piezometric head.

On the other hand, during a non-flood period, the subsurface impervious elements of FPM may cause damming of groundwater in the aquifer behind the FPM, with an unfavourable increase in the piezometric head permanently affecting the subsurface parts of civil structures in the area, or even with waterlogging of the terrain on the protected floodplain.

2.2. Hazardous Situations

A hazard is defined as a situation with the potential to cause undesirable effects. Here, this is induced by the action of groundwater on FPM elements and on the protected territory. The following situations may occur:

During a flood event:

- Flood protection structures are subjected to forces acting on their subsurface parts. In addition to earth pressure, forces caused by the groundwater underflowing the foundations must be taken into account. The most critical horizontal (F_h) and vertical (F_v) water pressure forces are shown in Figure 2a.
- An increase in the piezometric head in the confined aquifer behind the FPM may result in uplift acting on impervious fluvial topsoil (Figure 2b). Similarly, pressure due to the increase of the groundwater level (piezometric head) may affect the subsurface parts of the buildings with deep foundations (Figure 2c). Such uplift can cause ruptures in the topsoil and buildings, resulting in localized concentrated leakage, significant deformation of foundation slabs, or even global structural instability. This may also initiate waterlogging of the objects (Figure 2d).
- In cases when permeable soils crop out to the terrain, seepage may occur behind the FPM. This causes loading of soils by a pressure gradient, which may result in the internal erosion of susceptible soils (Figure 2d) in the form of external suffusion or boiling. These processes in the progression phase may often endanger the stability of the FPM.
- In case of long-term floods, in combination with the permeable aquifer, waterlogging of the area behind the FPM may occur due to seepage onto the terrain (Figure 2d).

During a non-flood period, the undesirable effect of impervious elements such as slurry walls may manifest itself:

- Damming of the groundwater level (GWL) in an aquifer behind the FPM (Figure 3a) may cause a significant permanent rise of groundwater levels, resulting in waterlogging of subsurface parts of buildings in the area.
- If groundwater resources occur behind the FPM, impervious subsurface elements may block the natural bank infiltration from a river and thus deteriorate the water source, respective to a decrease the yield of wells (Figure 3b). This may also result in a significant decrease of GWL in the protected area and cause unacceptable overloading of wells.

A list of potential hazards caused by changes in the groundwater regime due to flooding and the FPM is summarized in Table 1. In Table 1, the change of the groundwater regime is short-term (temporary from hours to single weeks) during the flood according to flood duration and long-term in cases when subsurface elements of the FPM permanently affect the groundwater flow.

Table 1. List of potential hazards caused by a change in the groundwater regime.

Period	Hazard	Potential Consequences
Flood	Temporary increased water pressure on subsurface parts of FPM	Loss of stability of FPM, flooding of protected area
	Temporary increased water pressure on aquifer topsoil behind FPM	Collapse of topsoil layer, internal erosion of subbase soil, collapse of FPM
	Temporary rise of water table/piezometric head in protected territory, seepage behind FPM on terrain, increased hydraulic gradients below FPM	Soil instability due to seepage, internal erosion, loss of stability of FPM
No flood	Temporary rise of water table in protected territory Permanent rise of groundwater table/piezometric head, damming due to subsurface elements of FPM	Temporary waterlogging of terrain behind FPM Permanent waterlogging of terrain and structures behind FPM, increased pressure on underground parts of structures
	Permanent reduction of bank infiltration due to impermeable subsurface parts of FPM	Reduction of water extracted from groundwater resources, groundwater level drawdown, overloading of wells

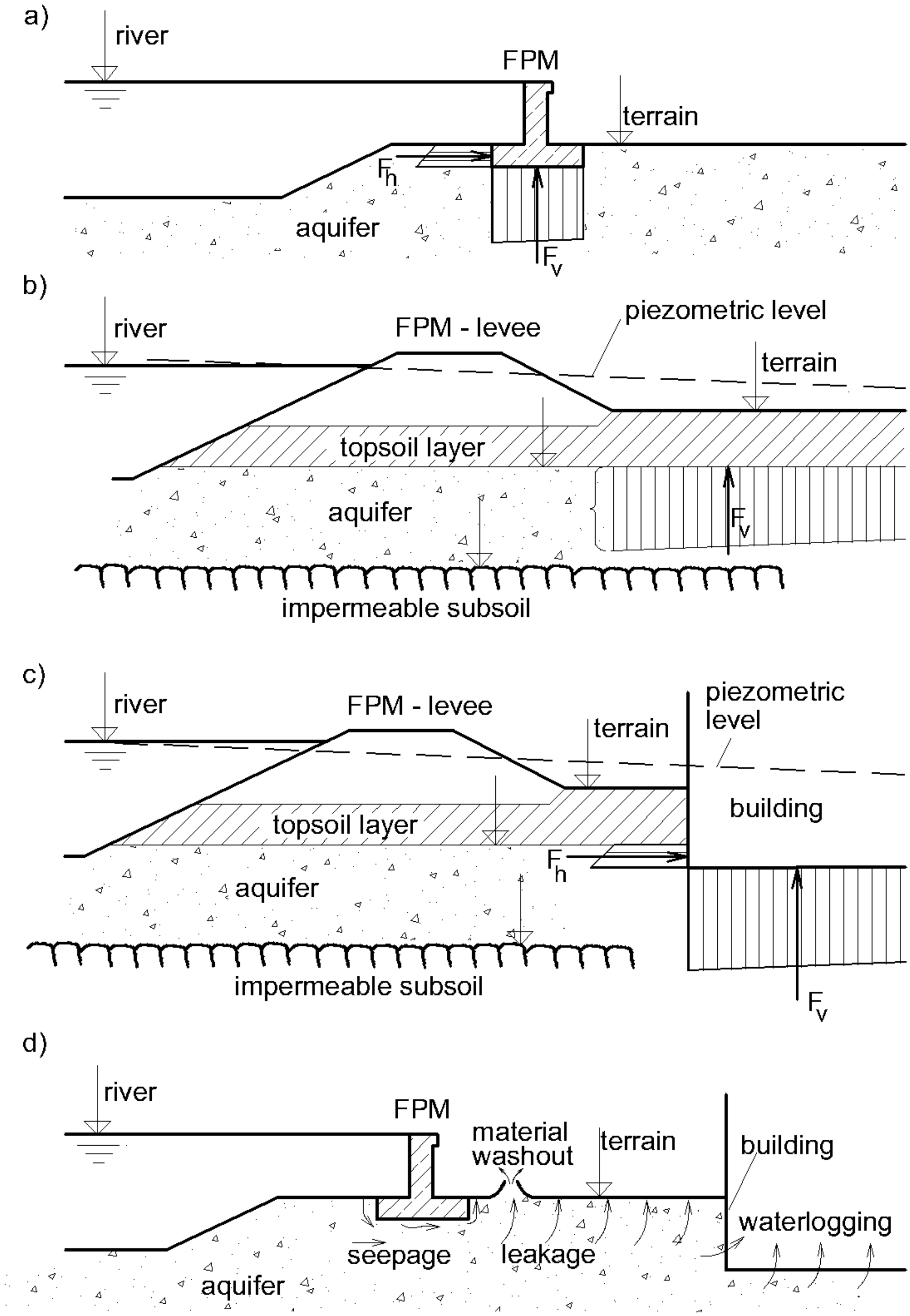

Figure 2. Hazards during a flood: (**a**) load on the foundations of the FPM, (**b**) uplift on the topsoil layer, (**c**) loading of the subsurface parts of civil structures behind the FPM, (**d**) seepage onto terrain, waterlogging, internal erosion of soils due to high hydraulic gradients behind the FPM.

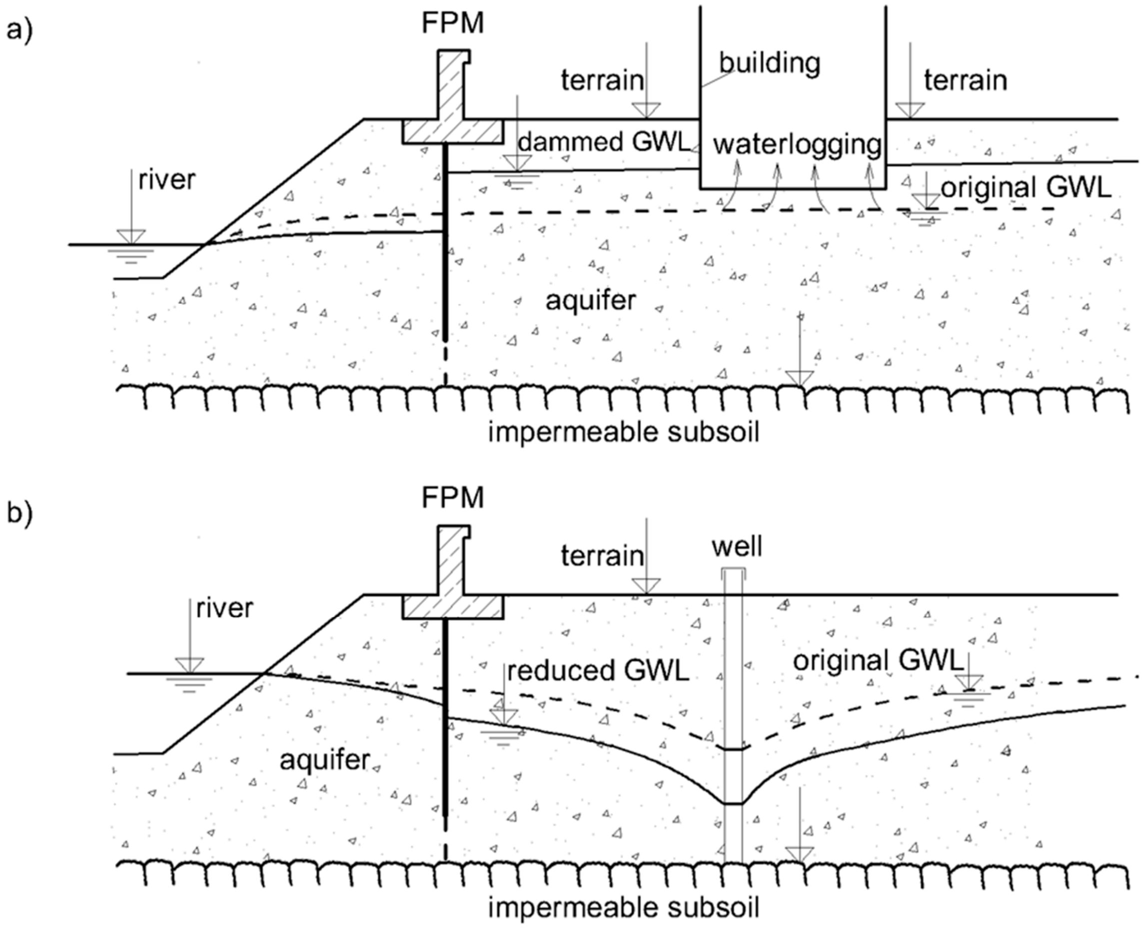

Figure 3. Hazards during a non-flood period: (**a**) damming of the groundwater on the protected area side, (**b**) effect on the yield of groundwater sources of subsurface parts of the FPM.

2.3. Hazard Quantification

Today, the quantification of individual hazard characteristics is carried out predominantly by groundwater flow models. The variables obtained as a result of hydraulic modelling are:

- piezometric head h;
- water pressure p, horizontal (F_h) and vertical (F_v) water pressure forces acting on the surface of subsurface structures, topsoil layer, and the FPM;
- pressure, or hydraulic gradient (grad p, grad h), which acts on the soil as a volumetric force and may cause its internal instability;
- waterlogging of the area is quantified by the affected area A, where water seeps onto terrain;
- seepage amount Q when dealing with pumped water from wells.

Generally, all hazard quantifiers are a function of the location (coordinates) and time. The spatiotemporal fields of respective variables (p, h, grad p, grad h, etc.) are determined by numerical modelling. A more detailed description of the models can be found in Section 3.

2.4. Data Acquisition

To ensure accurate modelling, it is crucial to acquire relevant data that may differ from those needed for analysing other types of floods. The geological structure and hydrogeological properties of the area of interest are of utmost importance, which may not hold true for "surface" floods. A brief overview of the individual data required and their acquisition is presented below.

Geographic and geodetic data describe terrain levels and provide information about structures within the studied area. The terrain levels are efficiently obtained via the combination of Digital Terrain Models (DTM) with more accurate geodetic land surveying. The data about structures should include the shape of subsurface structures, including the foundation depth (level), and preferably the type and material of the structure. Of special interest are linear conduits such as sewers of large diameters, integrated pipe galleries, underground railway lines, etc.

FPM design projects (floodwalls, flood levees) should be incorporated into terrain geometry. Subsurface elements such as slurry or cut-off walls and drainage systems must be taken into account.

Geological and hydrogeological data gained from geological surveying should provide information on local geological conditions and structures. Hydrogeological information should include a description of the groundwater regime (flow direction and amount, piezometric level in the aquifer, seepage amount), permeability values, and storage characteristics. These data are taken from the monitoring of observation boreholes, from pumping tests, and possibly from the determination of soil properties (grain size distribution, porosity, uniformity, etc.).

Hydrological and hydraulic data should specify water levels in surface water bodies (rivers, lakes), both during the non-flood period and during floods, in the form of flood hydrographs. The water levels which represent boundary conditions for seepage flow are frequently determined by open channel hydraulics methods.

Additional data should be obtained to provide information about existing water wells, pumping amounts, other agricultural drainage systems, etc.

Most of the data are usually available from administrative bodies that provide data to the public, including geological services and archives, hydrological services, and river authorities. In most cases, the required data have a spatial character and may be linked to spatial coordinates. For their analysis, pre-processing, and representation, the use of CAD and/or GIS tools is recommended.

Uncertainties in such input data produce uncertainties in the modelling results. These are discussed in Section 3.6.

3. Groundwater Flow Modelling

Numerical groundwater flow modelling has been a standard discipline in continuum mechanics since the early 1970s [15,46]. As the physical background, assumptions, and mathematical formulation are sufficiently described and discussed in the relevant literature, this text contains only a brief description and the general characteristics of individual models, with a focus on their use in practical applications.

3.1. Modelling Procedure and Types of Models

To assess the hazards mentioned in Section 2, models of the flow in the saturated zone are preferentially used. The modelling procedure comprises a set of the following standard steps:

- The description of a real system where the area of interest is identified, and management problems and potential hazards are formulated.
- The objectives of modelling have to be carefully defined together with expected outcomes (see Section 2). This involves the analysis of both flood and non-flood situations.
- The conceptual model consists of a set of assumptions related to the geometry, shape, and boundaries of the domain, as well as aquifer materials and their properties (homogeneity, isotropy, porosity, hydraulic conductivity, compressibility, etc.). According to the expected character of the flow, the dimension and time regime (steady, transient) of the model are defined (Table 2).
- The mathematical formulation (model) is represented by a set of governing equations, plus initial and boundary conditions.

- The computer code appropriate for the problem solution has to be selected [47–49]. Pre- and post- processing are necessary parts of the data analysis, preparation, and presentation. To this end, engineering approaches are combined with efficient post-processing methods which enable the display of spatial and temporal data using CAD systems and thematic maps within GIS tools.
- The numerical model should be subject to calibration and verification based on data from groundwater level observations and pumping amount measurements. The calibrated and verified model may be used for the simulation of scenarios that answer posed questions and achieve defined objectives.

Table 2. Summary of the application of groundwater flow models.

Problem	Type of Model	Solution Method
preliminary assessment of the propagation of a flood wave into an aquifer	1D—transient	analytical methods for simplified boundary and initial conditions, numerical methods
complex spatial assessment of flood wave propagation into a larger aquifer, assessment of piezometric head and pressure in the aquifer, assessment of local stability of the topsoil and structures behind FPM, delimitation of waterlogged areas	2Dh—transient	numerical methods
assessment of the effect of subsurface elements of FPM during non-flood periods, changes in the yield of affected water sources, piezometric head and pressure in an aquifer, assessment of the stability of structures behind FPM, hazard of waterlogging	2Dh—steady state	numerical methods
detailed assessment of the local conditions in the vicinity of FPM, stability of FPM and other structures for the peak flood water level scenario, assessment of non-flood scenarios	2Dv—steady state	numerical methods
solutions at places with complex geometrical conditions and a general flow direction, such as FPM that cross subsurface conduits, tunnels, etc.	3D—steady state	numerical methods

For the solution of individual cases, the selection of an appropriate type of model is crucial. This concerns the simplification of assumptions related to the spatial and time dimensions of the model. The following model types may be distinguished:

- one-dimensional (1D) groundwater flow model for cases where parallel seepage in a flat aquifer with small hydraulic gradients is expected (Dupuit assumption)—this model may be used for both confined and unconfined aquifers;
- two-dimensional model in the horizontal plane (2Dh) applicable for large and complex aquifers with small hydraulic gradients (Dupuit assumption)—this model may be used for both confined and unconfined aquifers;
- two-dimensional model in the vertical plane (2Dv), which can be used for parallel flow with significant variation in flow direction in the vertical plane, both for confined flow and flow with a phreatic surface;
- three-dimensional model (3D) for flow both in confined and unconfined conditions.

All of the models mentioned above may be conceived as steady (stationary) or dynamic (transient) according to the nature and regime of seepage. Generally, flow in the saturated zone is the subject of analysis.

In practical cases, the sequence of models used is usually as follows:

- preliminary analysis is carried out using a 1D model;
- complex analysis of flood propagation to the aquifer using a transient 2Dh model;
- modelling of the conditions during a non-flood period using a steady state 2Dh model;

- detailed analysis of conditions at the FPM using a steady state 2Dv model;
- if necessary, the detailed steady state 3D modelling of singularities, where no dimensional approximations exist, may be considered.

3.2. One-Dimensional Model

A one-dimensional transient model may be used for preliminary calculations at a small hydraulic gradient (the Dupuit theorem) and with approximately parallel flow. It can be used for the analysis of the propagation of a flood wave into an aquifer during a flood.

The governing equation holds [50]:

$$\frac{\partial}{\partial x}\left(T\frac{\partial h}{\partial x}\right) - S \cdot \frac{\partial h}{\partial t} + q = 0 \tag{1}$$

where T is aquifer transmissivity ($T = k \cdot b$ for confined aquifers, $T = k \cdot H$ for unconfined aquifers), k is hydraulic conductivity, b is the thickness of the confined aquifer, and H is the water depth of the unconfined aquifer. S is the storativity, which in the case of the confined aquifer is equal to the specific storage multiplied by aquifer thickness b, while in the case of the unconfined aquifer, it corresponds to the specific yield [15], and q is the linear source (e.g., infiltration at the unconfined aquifer).

The boundary condition (BC) expresses the known (prescribed) piezometric head during a flood (Dirichlet BC):

$$h(x,t) = \overline{h}(x,t) \tag{2}$$

For the initial conditions, it holds that:

$$h(x,0) = h_0(x) \tag{3}$$

The time-dependent boundary conditions (2) at the riverside comes from the water stages during a flood, which are derived from open channel hydraulics or measurements at gauging stations. The setting of the boundary condition and its location at the dry side of the FPM is more complicated. It is recommended that it be fixed sufficiently far from the river to eliminate its influence on the area close to the FPM. Another option in numerical modelling is to provide the computational (finite element, finite difference) elements adjacent to the BC with smaller hydraulic conductivity to attenuate their effect on the seepage conditions in the aquifer close to the FPM.

The result of the calculations is the piezometric head, or phreatic surface, as a function of the horizontal coordinate x and time t. In this model, the pressures, the hydraulic, and pressure gradients derived from piezometric heads are not relevant for further detailed analysis and the assessment of the consequences for single structures. As mentioned above, this model serves predominantly to provide preliminary information about the progression of a flood to an aquifer.

1D modelling, due to the very small computation time involved, often includes the sensitivity analysis of input parameters such as hydraulic conductivity and storativity, and is also performed with the aim of setting the distance of the dry-land boundary condition. The 1D model provides the first idea about the groundwater regime which is to be investigated in more complex models. It enables the setting of boundary conditions and gives information about the most unfavourable combination of input parameters. It also enables the preliminary calibration of model parameters if data from groundwater regime measurements are available.

An example concerning the time evolution of the piezometric head in an aquifer adjacent to the Vltava River in Prague during a flood in 2002 can be seen in Figures 4 and 5. It can be seen that the peak piezometric head follows the peak of the water level in the Vltava River (boundary condition), with a certain degree of attenuation and time shift. The rate of propagation depends on the hydraulic conductivity of the aquifer and on the storativity. As a rule, in the case of an unconfined aquifer, the seepage propagation is considerably slower than in the case of a confined one as the unsaturated soil should firstly be saturated before the phreatic surface can rise further in the aquifer.

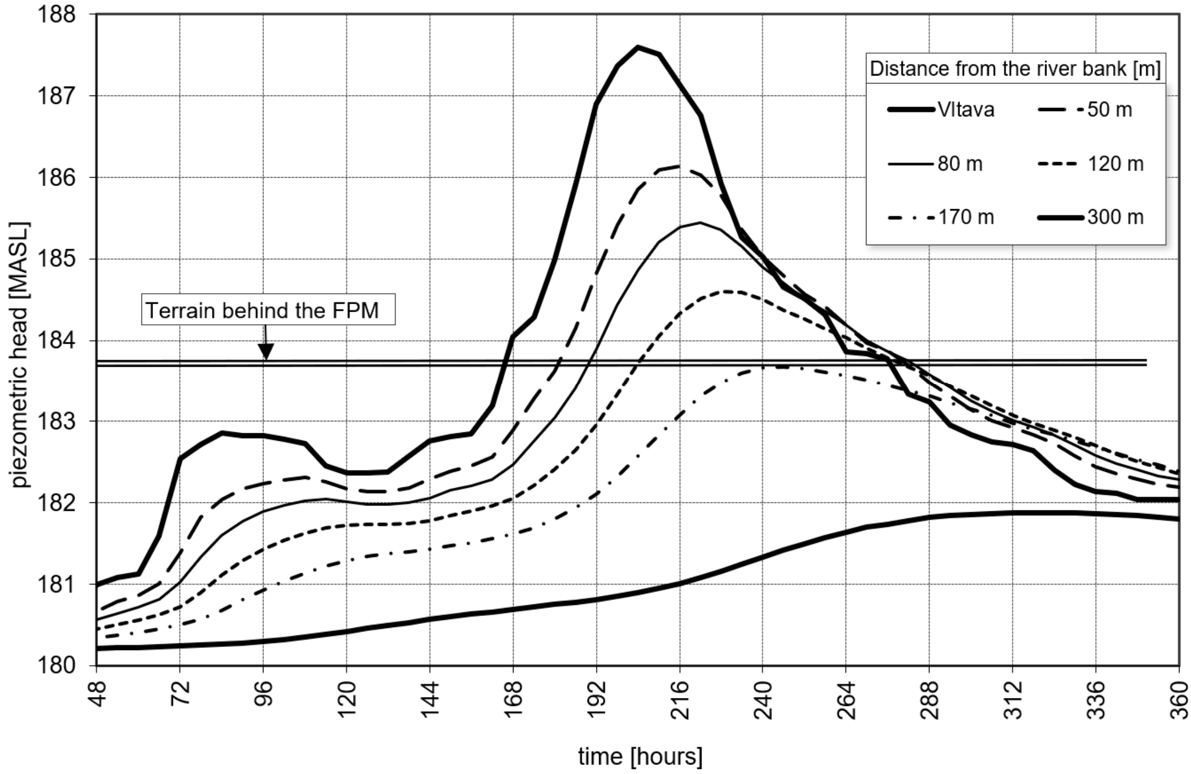

Figure 4. Flood wave propagation into an aquifer–piezometric head at selected distances from the Vltava river bank.

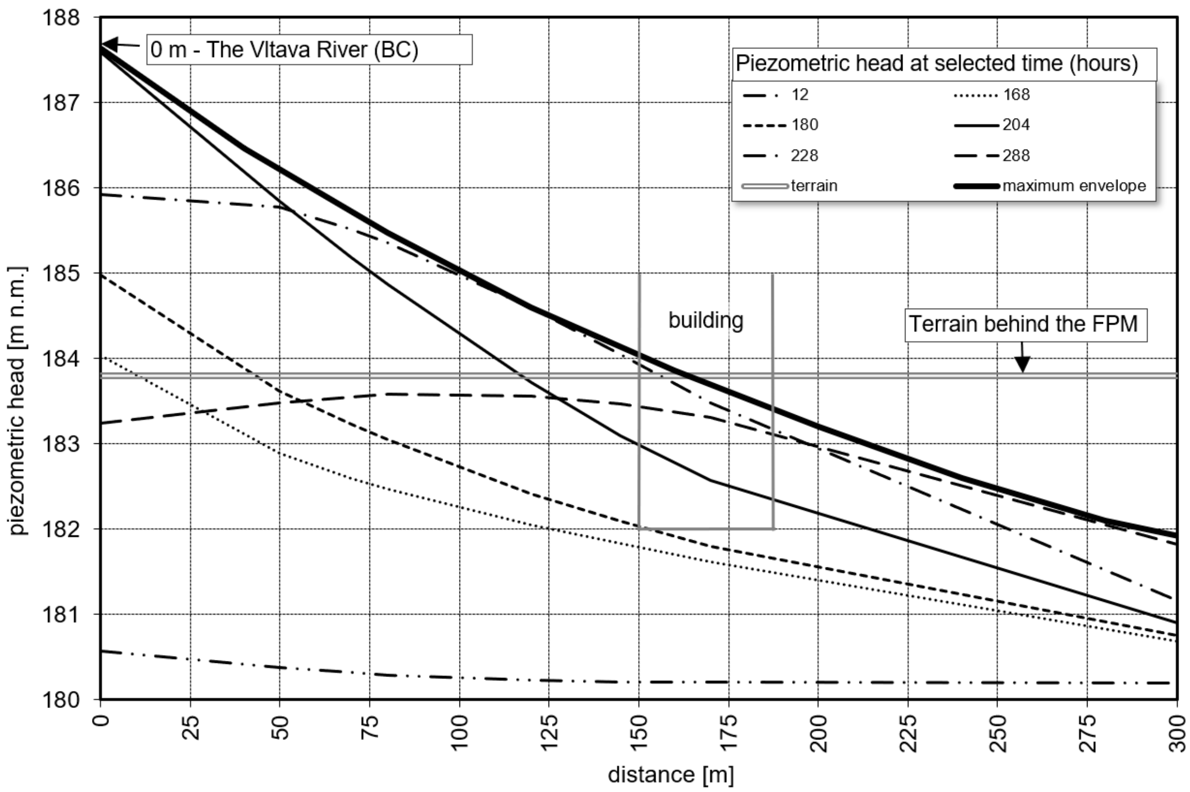

Figure 5. Flood wave propagation–piezometric head at selected time instants.

3.3. 2Dh Model of Flow in a Horizontal Plane

A 2Dh model of groundwater flow in a horizontal plane is used, as in the case of the 1D model, to simulate the propagation of a flood wave into an aquifer during a flood, and for the assessment of the effect of the FPM on the groundwater regime during a non-flood period. Flow is expected in both confined and unconfined complex aquifers at a relatively small hydraulic gradient (the Dupuit theorem). The governing equation holds [15]:

$$\frac{\partial}{\partial x}\left(T_x\frac{\partial h}{\partial x}\right) + \frac{\partial}{\partial y}\left(T_y\frac{\partial h}{\partial y}\right) - S\cdot\frac{\partial h}{\partial t} = 0 \tag{4}$$

where T_i is aquifer transmissivity (this generally may differ in two directions; however, in practice, isotropy in the horizontal plane is acceptable). Other variables are analogical to the ones described below Equation (1).

The boundary condition of the first type (Dirichlet) prescribes the following piezometric head:

$$h(x,y,t) = \overline{h}(x,y,t) \tag{5}$$

where $\overline{h}(x,y,t)$ is the known piezometric head along the boundary, which usually follows the bank of the open channel. The location of the boundary behind the FPM may be derived from the 1D sensitivity analysis or from hydrogeological observations.

At the remaining domain boundary, the prescribed flux (Neumann BC) may be implemented:

$$T_x\frac{\partial h}{\partial x}n_x + T_y\frac{\partial h}{\partial y}n_y = q_p \tag{6}$$

where n_x, n_y are direction cosines related to the outer normal vector to the boundary with prescribed flux q_p (per unit width of the boundary). At the "no flow" boundary, Equation (5) may be applied with q_p = 0. This kind of BC is applied along expected no-flow lines (perpendicular to groundwater table contours), which are usually located rather far from the area of interest.

The initial condition expresses the known piezometric head h_0 over the flow domain at t = 0:

$$h(x,y,0) = h_0(x,y) \tag{7}$$

The known piezometric head may be interpreted from field measurements or taken from results obtained by a calibrated steady state solution corresponding to the conditions before the flood.

Similarly, as with the 1D model, the 2Dh model may be used to analyse the propagation of a flood wave in an open channel into spatially more extensive and complex aquifers and seepage conditions. Here, the resulting piezometric head enables the assessment of pressure in the aquifer, the local stability of the topsoil and structures behind the FPM, and the delimitation of waterlogged areas behind the FPM (Figure 2b–d).

This kind of model is also suitable for the modelling of non-flood scenarios to assess the effect and possible consequences of subsurface elements of the FPM (such as deep foundations of floodwalls, slurry, or sheet pile walls). The effects may be as follows:

- Subsurface elements of the FPM may unacceptably increase the water level in the aquifer behind the FPM (Figure 3a), increase the water pressure on the floors and walls of cellars, and cause dampness of walls and even waterlogging of the terrain. The situation may be crucial in case of the infiltration of rainwater in urban areas behind the FPM.
- If riverbank infiltration supports the water supply provided by wells close to the riverbank, subsurface elements of the FPM may reduce the yield of affected water sources (Figure 3b).

The results of the simulations can be used as the basis for the structural design of subsurface elements, for the possible assessment of semi-pervious slurry walls, the conceptual location of remedial measures such as drainage, etc. Conceptual proposals are developed into final designs with the use of detailed 2Dv or 3D models. The resulting piezometric heads in a more extensive flow domain may be used for the delimitation of boundary conditions for more detailed 2Dv or 3D models.

The results may be depicted by a time series of the piezometric head at a given location (such as in Figure 4), or by piezometric levels along a selected profile at given points in time (Figure 5). This is illustrated here by a ground plan showing maximum levels of the piezometric head in the aquifer during a flood (Figure 6a) and differences between the piezometric head and the terrain-waterlogged areas (Figure 6b).

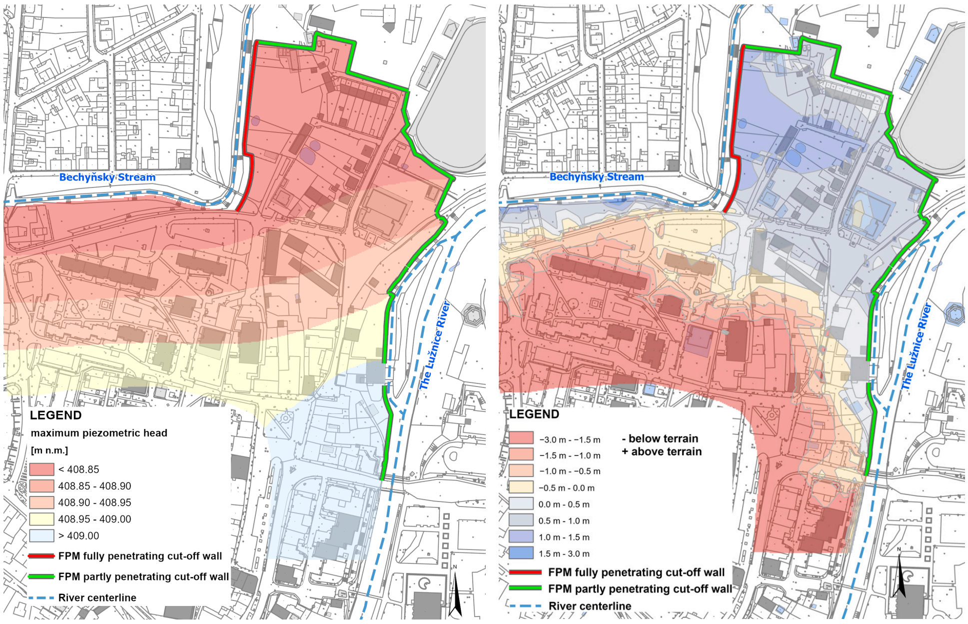

Figure 6. (**a**) Maximum levels of piezometric head in a confined aquifer during a flood, (**b**) Difference between piezometric head and terrain level (zones at risk with "-").

During the no flood period, interaction between surface and subsurface water occurs in the form of either drainage flow to the stream or infiltration to an aquifer from the stream. It is usually inappropriate to cause the complete closure of the aquifer with a completely penetrating cut-off wall in the impermeable layer. Based on model calculations, it is usually possible to propose partly penetrating cut-off walls, which ensure the reliable function of flood protection measures (often in combination with an efficient drainage system; see below), and at the same time, maintain the connection of the stream to the aquifer. However, sometimes it is not possible to protect an area against waterlogging during a flood.

In Figure 6, the area protected against floods is located between a local stream named Bechyňsky stream (on the left) and the River Lužnice (on the right). The confined aquifer communicates with both streams; at the FPM line, the sub-base is provided by a fully penetrating slurry wall (red) and a partially penetrating wall (green). In Figure 6a, the maximum piezometric head during the flood taken from the dynamic 2Dh model is shown at the protected area. To get an idea about the topsoil potentially endangered by uplift (see also Figure 2b), the differences between the maximum piezometric head and the terrain (taken from DTM) have been processed (Figure 6b).

In case of a transient solution, it is possible to visualize the propagation of the piezometric head into the aquifer in selected sections, as it was with the 1D results (Figures 4 and 5).

A specific situation may arise in the case of the FPM. In this case, the situation during the non-flood period was studied. In Figure 7, the protected area is located between the original river and a headrace to the south with a significantly higher water level. Because of this, the "natural" groundwater tends to infiltrate from the headrace and drain into the original watercourse (Figure 7a). When the FPM are applied, subsurface anti-seepage elements are needed to prevent extensive waterlogging of the protected area. At the same time, it is necessary to keep the groundwater at the prescribed level to provide domestic water supply wells with a sufficient amount of groundwater during non-flood periods. Two variant solutions were created, the first with completely penetrating slurry walls around the entire perimeter of the area (Figure 7b), and the second with combined partially and fully penetrating walls (Figure 7c). With the first variant, the slurry wall provides reliable protection against seepage during flooding, though artificial infiltration behind the FPM is needed. It is proposed that this should occur from the headrace canal (from the south). In the case of partially penetrating walls, no additional water supply is needed (Figure 7c). However, the threat of waterlogging of the area is dealt with by a peripheral drain located behind the FPM.

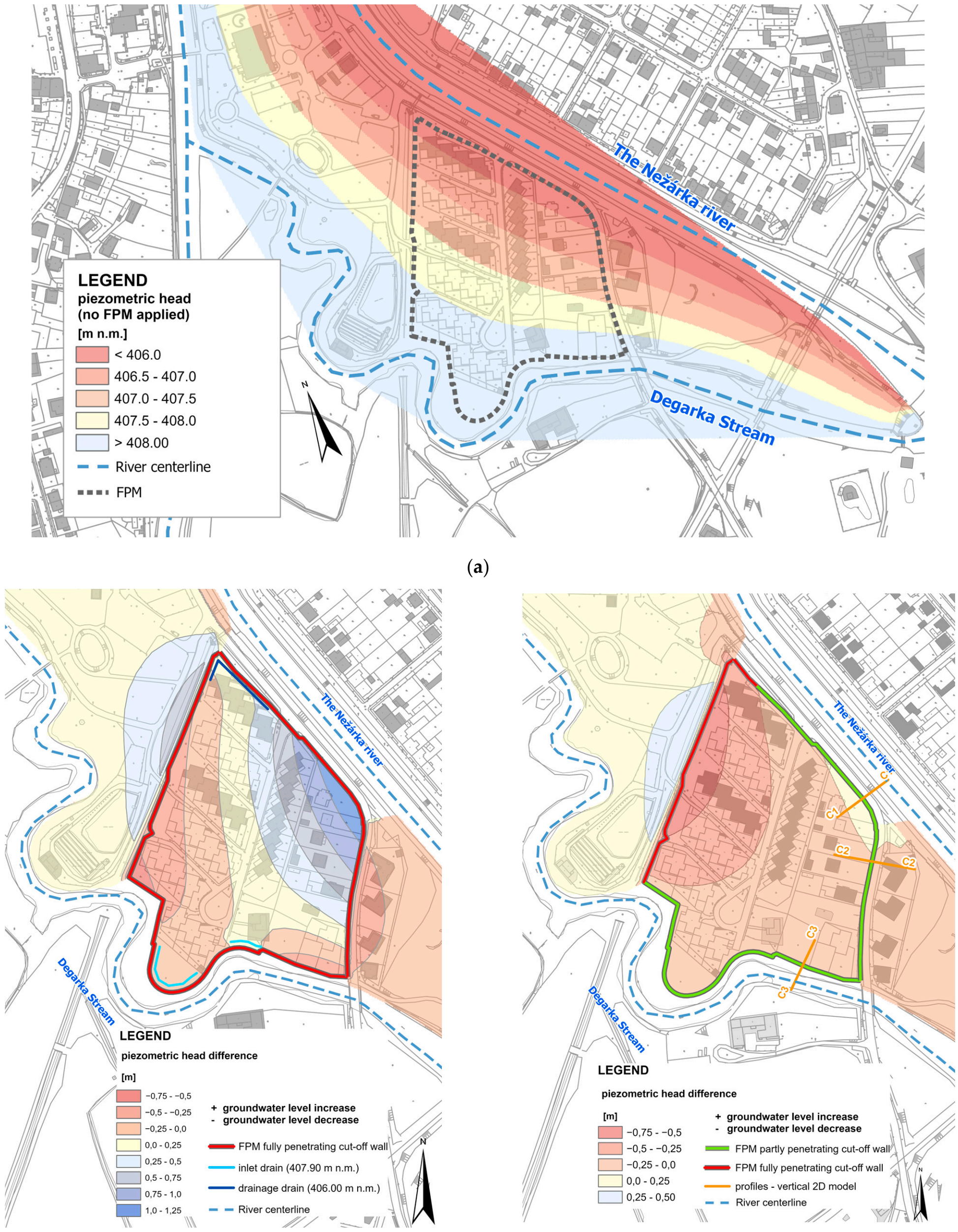

(a) (b) (c)

Figure 7. (**a**) Non-flood FPM applied; (**b**) Complete enclosure of the aquifer with a fully penetrating cut-off wall, with measures taken to allow groundwater to flow in and out; (**c**) Extensive partly penetrating cut-off wall.

The examples shown in Figures 6 and 7 come from the locality of Veselí nad Lužnicí in the Czech Republic.

Another interpretation is possible via what can be termed the "over-design factor" *OF*, which is the equivalent of a traditional safety factor that already takes into account uncertainties in load and resistance by incorporating them into the design [36,51,52]. Safety against uplift is achieved if $OF \geq 1$. In the area where $OF < 1$, measures have to be adopted, e.g., raising the terrain level or using relief wells.

In Figure 8, the over-design factor is used to depict an area endangered by uplift in an industrial zone in the vicinity of the city of Brno. This area is protected from floods coming from the Svratka river (left). The over-design factor is related to the maximum piezometric head taken from the dynamic 2Dh model.

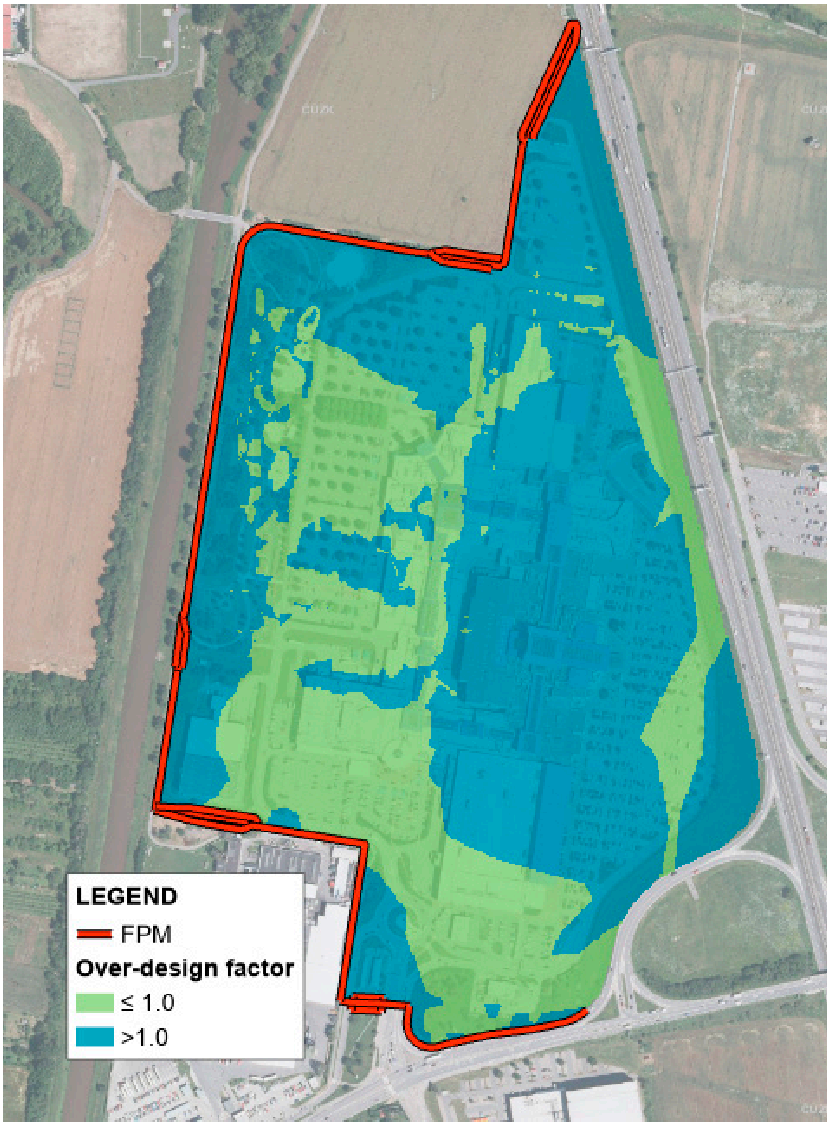

Figure 8. Map of overdimensioning factor *OF*.

3.4. 2Dv Model of Flow in a Vertical Plane

A 2Dv model of flow in a vertical plane is used in cases in which the components of flow in the direction of the longitudinal axis of the FPM can be neglected. To assure the adequate "safety" of the results, the use of a steady state approximation for the most unfavourable conditions is recommended. This model can be used for confined aquifers, phreatic surfaces, or mixed flow conditions. The governing equation for a non-homogeneous anisotropic aquifer and steady state seepage holds:

$$\frac{\partial}{\partial x}\left(k_x \frac{\partial h}{\partial x}\right) + \frac{\partial}{\partial z}\left(k_z \frac{\partial h}{\partial z}\right) = 0 \tag{8}$$

Dirichlet and Neumann boundary conditions are analogical with Equations (5) and (6):

$$h(x,z) = \overline{h}(x,z) \tag{9}$$

$$\left(k_x \frac{\partial h}{\partial x}\right) n_x + \left(k_z \frac{\partial h}{\partial z}\right) n_z = q_p \tag{10}$$

On a phreatic surface with a steady state flow, two boundary conditions may be applied. When zero pressure is applied on the phreatic surface, Equation (9) transfers to:

$$h(x,z) = z_p(x) \tag{11}$$

At the same time, Equation (10) with q_p = 0 holds on the phreatic surface.

On the seepage face, it holds that:

$$h(x,z) = z_s(x) \tag{12}$$

where z_p and z_s are the phreatic surface level and seepage face, respectively [15]. To find the free water level and seepage face, special iterative techniques may be used [47].

The concept of the phreatic surface is pertinent in the case of an unconfined aquifer where toe drains are proposed to trap seepage below the FPM. When flood levees are from relatively impermeable soils, the presence of a phreatic surface in the levee is disputable, since namely in small and average-sized streams, the flood duration is usually smaller than the duration of seepage progression to the downstream slope. However, considerable seepage through the levee may be expected when inappropriate permeable material is used for levee construction. This may be the case with older existing levees, e.g., the levees along the Danube and its tributaries, which were constructed almost 200 years ago.

In the case of a confined aquifer (Figure 2b,c), no seepage occurs. If one is not sure about the seepage regime, it is recommended that the strategy with a phreatic surface be applied. Most of the existing computer codes, such as Galavi [47] or GMS [48], accommodate and solve the problem as combined phreatic/confined flow.

In 2Dv models, the primary variable is the piezometric head, from which pressure, hydraulic and pressure gradients, and seepage amount per 1 metre width of the FPM line can be calculated.

In Figures 9 and 10, the complicated flow in the vicinity of the FPM in the city of Brno is depicted. The houses and large sewer main are located behind the floodwall. Due to potential waterlogging in the non-flood period, the slurry wall must not completely penetrate the impermeable subbase layer. To prevent waterlogging of the terrain and the effects of uplift on cellars and sewer pipes during a period of flooding, the drainage pipe is located just behind the floodwall in the granular backfill of the sewer main. In Figure 9, the overall layout of the locality is shown via a cross section. Here, the piezometric head contours and water table drawn down by the drain are shown. In Figure 10, hydraulic gradients and seepage flow directions are depicted.

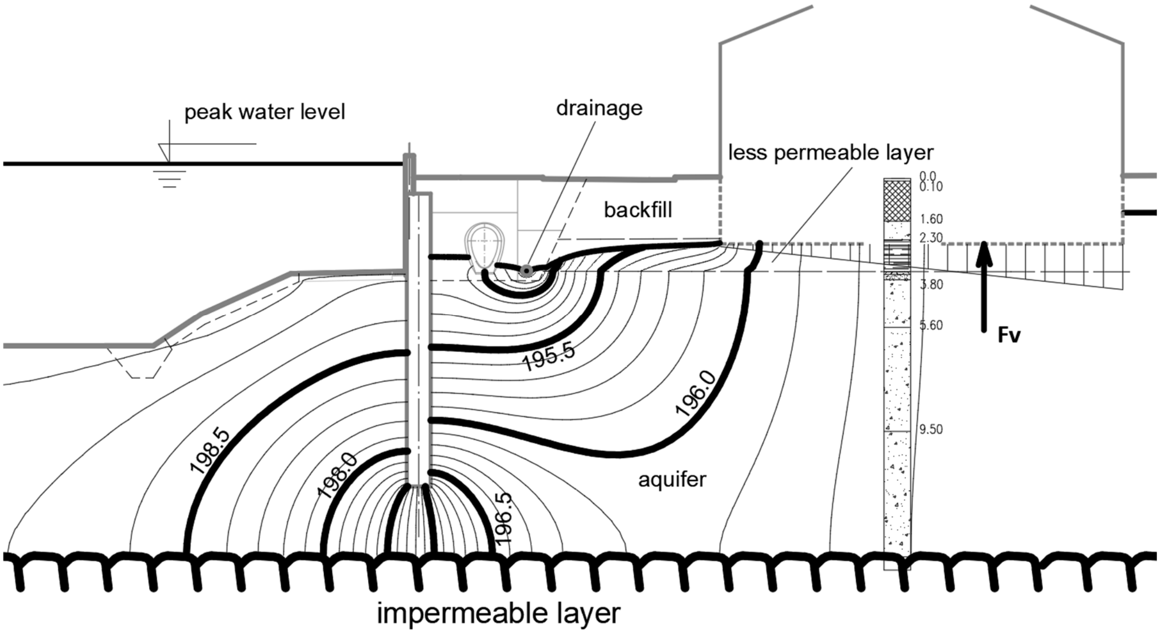

Figure 9. Contours of the piezometric head in a cross section of FPM.

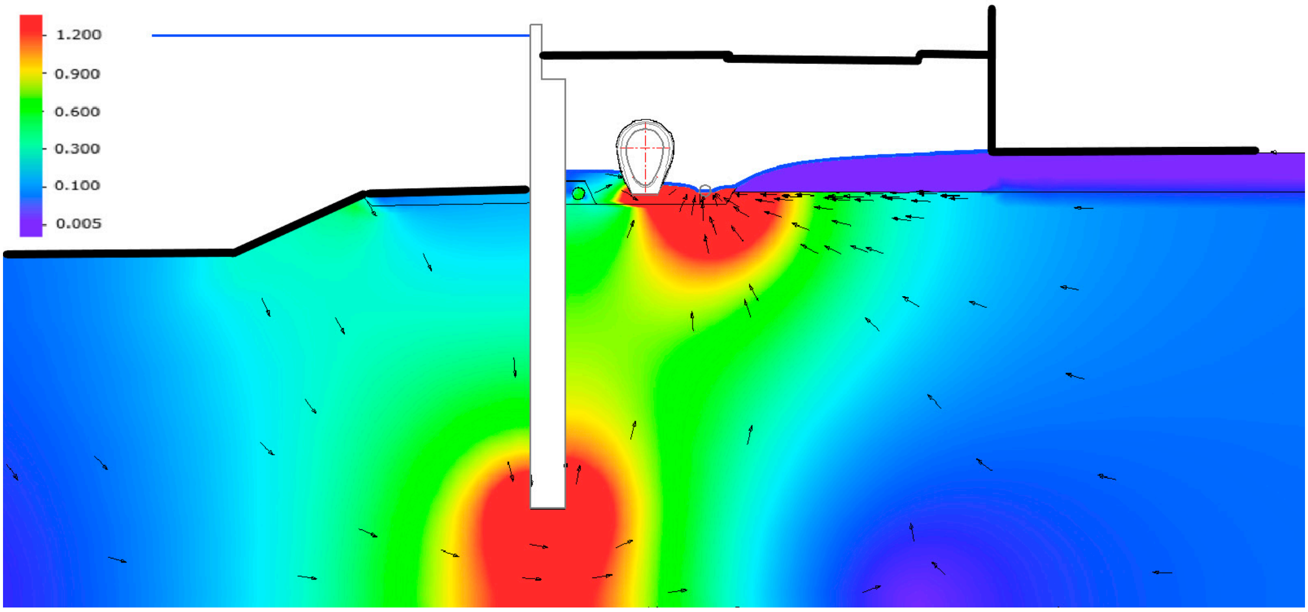

Figure 10. Hydraulic gradients in a cross section of FPM (same as Figure 9). Arrows represent groundwater flow direction.

3.5. 3D Model

3D models are used particularly for solving complicated details where the approximations mentioned above are not acceptable. For the assessment of flood protection measures and other affected structures, it is usually sufficient to apply a steady-state solution corresponding to the most unfavourable conditions selected for individual scenarios. The governing equation for anisotropic and nonhomogeneous materials holds:

$$\frac{\partial}{\partial x}\left(k_x \frac{\partial h}{\partial x}\right) + \frac{\partial}{\partial y}\left(k_y \frac{\partial h}{\partial y}\right) + \frac{\partial}{\partial z}\left(k_z \frac{\partial h}{\partial z}\right) = 0 \tag{13}$$

Boundary conditions are analogical to the 2Dv model. Dirichlet BC:

$$h(x,y,z) = \overline{h}(x,y,z) \tag{14}$$

At the boundary with prescribed flux, the Neumann condition holds:

$$\left(k_x \frac{\partial h}{\partial x}\right) n_x + \left(k_y \frac{\partial h}{\partial y}\right) n_y + \left(k_z \frac{\partial h}{\partial z}\right) n_z = q_p \tag{15}$$

On the phreatic surface with a steady state flow, two boundary conditions may be applied. The first one may be expressed as follows:

$$h(x,y,z) = z_p(x,y) \tag{16}$$

while the second one corresponds to Equation (15) with $q_p = 0$.

At the seepage face, BC has the form:

$$h(x,y,z) = z_s(x,y) \tag{17}$$

Most computer codes solve phreatic flow seepage using the concept of an unsaturated zone, where the saturated domain corresponds to the pore pressures $p \geq p_a$, where p_a is atmospheric pressure, or $p \geq 0$ if the atmospheric pressure is used as the reference pressure.

As mentioned above, 3D models are used in cases where dimensional simplifications are not feasible. There is a large variety of practical situations where the flow direction is quite general and simpler models (1D, 2Dh, 2Dv) are not applicable. Such flow may occur in complex geological conditions combined with spatially variable civil structures interfering with the flow domain [53–55]. Due to the large number of computational nodes in a 3D model, the flow domain size is usually minimized while boundary conditions are determined by a preliminary simplified analysis using 2D models. During modelling, it is feasible to divide the flow domain into homogeneous blocks (macroelements; see Figure 11), and to apply the computational mesh (e.g., finite elements) later on.

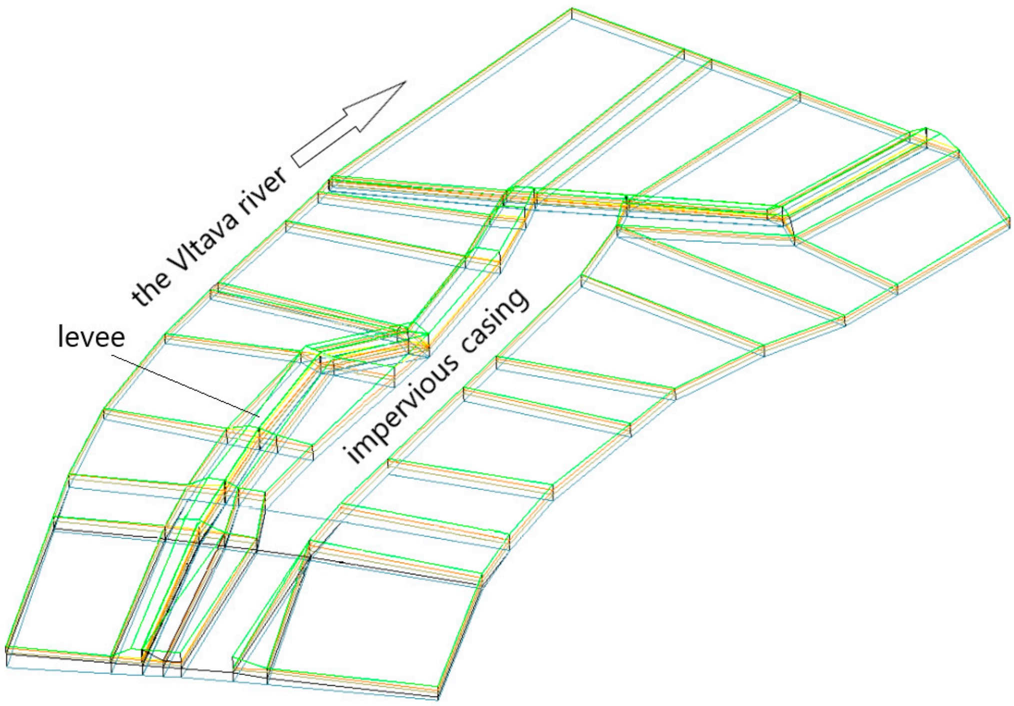

Figure 11. Diagram of layered 3D macroelements. Different colours represent soil layers interfaces.

The following example concerns the complex seepage flow below the levee, which interferes with subsurface elements of the tunnel crossing the Vltava river (Prague) and gradually rises out to the terrain in the protected area behind the levee. In Figure 11, a layered scheme of macroelements is depicted. These macroelements correspond to geological and construction layers and are further meshed by finite elements with a size of 0.5 m, which ensures the accuracy of the results is sufficient. Figure 12 shows a comparison of piezometric heads for various geological conditions, i.e., an aquifer overlaid by relatively impervious topsoil (a) and surface layers consisting of anthropogenic backfill (b). In Figure 13, a detail of a levee with a descending tunnel is depicted for scenario (b).

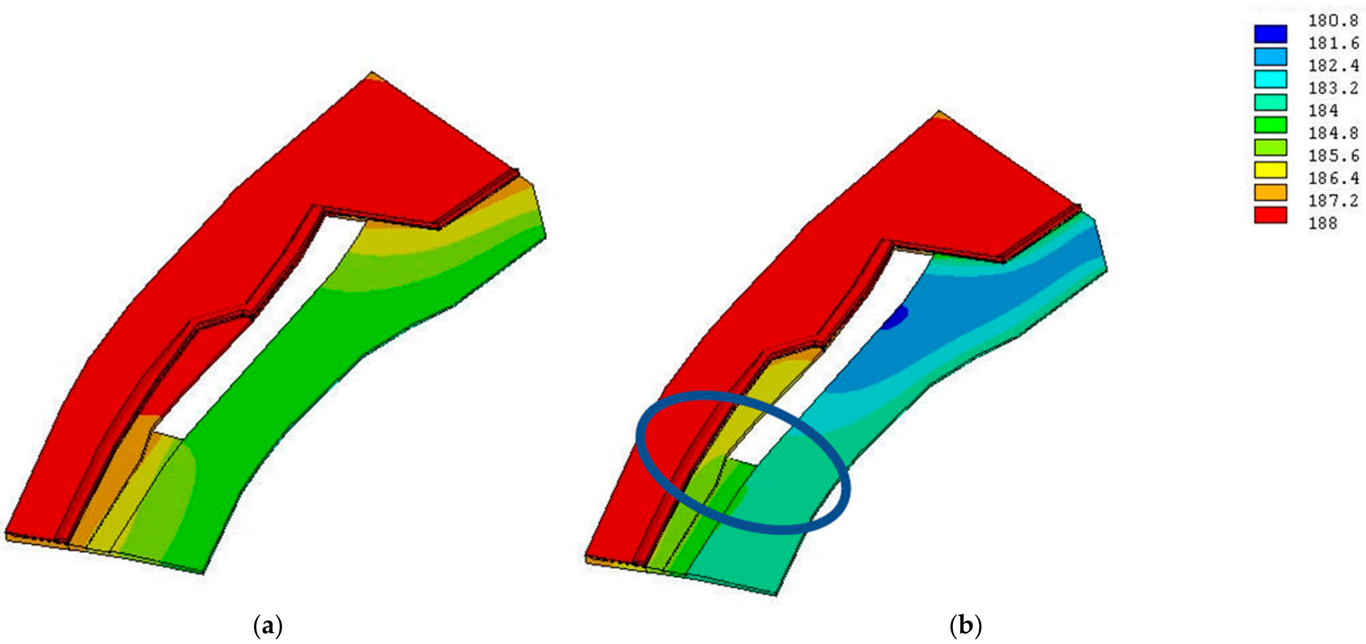

Figure 12. Comparison of piezometric heads on the base of a surface layer: (**a**)—only impervious topsoil, (**b**)—anthropogenic layer on the surface. Blue ellipse indicates detail of a levee with the descending tunnel ramp shown in Figure 13.

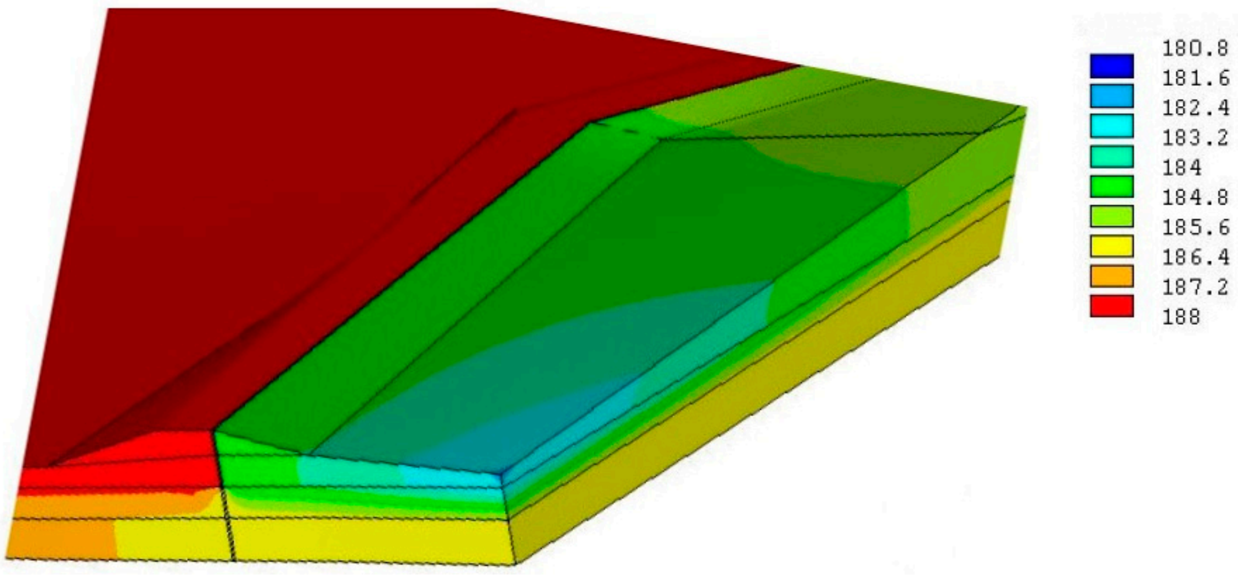

Figure 13. Detail of a levee with the descending tunnel ramp; scenario B according to Figure 12.

It is obvious that the interpretation of 3D results is difficult and should be processed via layers (Figure 12) and selected sections (Figure 13) of the 3D domain. Here, the pre- and post-processing ability of the computed code (e.g., [49]) is crucial.

3.6. Discussion of Uncertainties

In case of groundwater flow modelling, uncertainties relate particularly to:

- The geological composition of the area, such as the thickness of individual layers (aquifer, topsoil, etc.), which is usually derived from a limited number of boreholes or pits;
- limited understanding about overall hydrogeological and hydrological conditions, i.e., time-dependent groundwater flow regime, the direction and amount of groundwater flow, inflows and infiltration to an aquifer—the uncertainties are governed by the extent of monitoring network and frequency of readings;
- the knowledge about geological and hydrogeological properties of topsoil and aquifer soils, namely granulometry, porosity, hydraulic conductivity, and storativity, which are derived from laboratory and field testing, but in many cases only use empirical formulae supplemented by single hydraulic tests (pumping tests);
- the rate of interaction between the river and aquifer, which may be influenced by local clogging;
- boundary conditions, both at the riverside and behind the FPM, are derived from flood hydrographs which are not routinely statistically assessed in terms of their shape and flood volume;
- infiltration rates during the simulated event.

While the geometrical characteristics of the geological layers may differ in metres (tens of %), permeability and storage characteristics may be subject to degrees of uncertainty that are often very large (several orders). To reduce the effect of uncertainties, the following techniques may be recommended.

A sensitivity analysis is recommended for assessing how uncertainties in input variables influence uncertainties in output variables. Sometimes the impact of parameters such as hydraulic conductivity, transmissivity, storativity, etc., may be qualitatively estimated from the governing equations.

The reliability of a model may be significantly increased by careful calibration and verification. During the calibration, a unique set of model parameters is found that provides a good description of the system's behaviour, i.e., agreement with the piezometric head, yields, and other variables measured in the field.

A general engineering approach is to set "sensitive" characteristics and parameters so as to ensure conservative ("safe") results are obtained. For example, the rate of the rise in the piezometric head in the aquifer is greater with higher hydraulic conductivity (transmissivity) and smaller storativity.

Better information on the effect of uncertainties can be provided by the application of interval algebra or by statistical modelling procedures. However, in groundwater flow modelling, the stochastic modelling approach has not yet become a tool used routinely by modellers on a regular basis [56]. This is mostly due to the insufficient and poor geological and hydrogeological data that is available. In the case of stochastic studies, only single parameters are considered to be uncertain [57].

The simplifications of model dimensions and dynamics are related to the nature of the problem, the aims of modelling, and the shape and arrangement of the flow domain. Special attention should be paid to the analysis, graphical presentation, and interpretation of hazards using contemporary GIS and CAD systems. These are summarized in Table 3.

Table 3. List of potential hazards caused by a change in groundwater regime.

Period	Hazard	Interpretation	Figure
Flood	Increased water pressure on subsurface parts of FPM and structures behind FPM, detailed analysis	Map of pressure head, safety factor, cross sections with piezometric contours, pressure diagrams	Figures 2a,c, 5, 8 and 9
	Increased water pressure on aquifer topsoil behind FPM	Flood wave propagation diagrams, maps of piezometric head, uplift pressures, safety factor	Figures 2b, 4, 5, 6, 7a, 8, 12 and 13
	Rise of piezometric head in protected area, seepage on terrain	Flood wave propagation diagrams, cross section with piezometric contours and hydraulic gradients	Figures 4, 5, 9 and 10
	Temporary rise of water table in protected territory	Flood wave propagation diagrams, map of maximum piezometric head differences, map of waterlogged area	Figures 4, 5 and 6a
No flood	Rise of groundwater table/piezometric head, damming due to subsurface parts of FPM	Map of piezometric head differences and terrain, differences before and after construction of FPM	Figures 6b and 7
	Permanent reduction of bank infiltration due to impermeable/semipermeable subsurface parts of FPM	Map of differences in phreatic/piezometric surface, cross section through wells, drop in yield	Figures 3, 6b, and 7b,c

4. Conclusions

The paper summarizes the problems and techniques related to the modelling of groundwater flow impacts and hazards related to fluvial floods.

Two typical scenarios are discussed, namely a flood situation and a non-flood period. In all cases, the structural safety of the FPM and affected civil structures must be guaranteed. Experience shows that when inhabitants are affected, non-flood periods are more sensitive than relatively short periods of flooding. This namely concerns cases when waterlogging and similar harm to inhabitants and civil structures may occur. In these cases, the modelling results should be "safer" and technical proposals more robust. Moreover, in urban areas, technical measures often interfere with existing infrastructure placed alongside rivers, such as roads, subsurface water and sewer mains (Figure 9), electric linings, optical fibre cables, etc.

The presented study aims to fill the gap in a rigorous classification of groundwater hazards due to fluvial floods and the arrangement of the FPM. The novelty of the study lies in a formalised analysis of the technical aspects of groundwater hazards related to floods.

It can be seen that flood-protection problems related to groundwater are based on traditional groundwater flow modelling techniques. However, special site-specific approaches are necessary in the case of hazard identification and quantification, the selection of an appropriate groundwater flow model, and the presentation and interpretation of modelling results.

Based on the results obtained, technical measures for the attenuation of hazards can be proposed, such as the appropriate type and arrangement of slurry walls, FPM foundations, drainage systems, etc.

The paper summarizes experience obtained over 30 years of groundwater flow modelling related to the FPM design and assessment in the territory of the Czech Republic, Slovakia, and Austria.

Author Contributions: J.Ř.: Conceptualization, Methodology, Supervision, Writing—original draft, validation; T.J.: Conceptualization, Formal analysis, Investigation, Mapping, Writing—original draft and editing; D.D.: Investigation, Validation, Mapping, Writing—review and editing. All authors have read and agreed to the published version of the manuscript.

Funding: This research was funded by the Technology Agency of the Czech Republic, project number TH4030087 and Internal grant agency of the Brno University of Technology, project number FAST-S-23-8233.

Data Availability Statement: Not applicable.

Conflicts of Interest: The authors declare no conflict of interest. The funders had no role in the design of the study; in the collection, analyses, or interpretation of data; in the writing of the manuscript; or in the decision to publish the results.

References

1. Robins, N.S.; Finch, J.W. Groundwater flood or groundwater-induced flood? *Q. J. Eng. Geol. Hydrogeol.* **2012**, *45*, 119–121. [CrossRef]
2. CIRIA. *The International Levee Handbook*; U.S. Army. Corps of Engineers: Washington, DC, USA, 2013; 1332p.
3. Miroslaw-Swiatek, D.; Popielski, P.; Sliwinski, P.; Cwalina, T.; Skutnik, Z. Analysis of factors influencing levee safety using the DEMATEL method. *PLoS ONE* **2021**, *16*, e0255755. [CrossRef] [PubMed]
4. MacDonald, D.; Dixon, A.; Newell, A.; Hallaways, A. Groundwater flooding within an urbanised flood plain. *J. Flood Risk Manag.* **2012**, *5*, 68–80. [CrossRef]
5. Zhou, Y.; Li, W. A review of regional groundwater flow modelling. *J. Geosci. Front.* **2011**, *2*, 205–214. [CrossRef]
6. MacDonald, D.M.J.; Bloomfield, J.P.; Hughes, A.G.; MacDonald, A.M.; Adams, B.; McKenzie, A.A. Improving the understanding of the risk from groundwater flooding in the UK. In Proceedings of the Floodrisk 2008, European Conference on Flood Risk Management, Oxford, UK, 30 September–2 October 2008; CRC Press: Leiden, The Netherlands.
7. Environment Agency. *Making Space for Water, Groundwater Flood Records Collation, Monitoring and Risk Assessment*; Extended Report (Chalk Aquifers), Jacobs, Report to Environment Agency; Environment Agency: Bristol, UK, 2006; 187p.
8. Adams, B.; Bloomfield, J.P.; Gallagher, A.J.; Jackson, C.R.; Rutter, H.K.; Williams, A.T. An early warning system for groundwater flooding in the Chalk. *Q. J. Eng. Geol. Hydrogeol.* **2010**, *43*, 185–193. [CrossRef]
9. Chromá, K.; Brázdil, R.; Dolák, L.; Řehoř, J.; Řezníčková, L. Documentary data in the study of fatalities caused by meteorological and hydrological events: The Czech Republic, 1964–2019. In Proceedings of the EGU General Assembly 2020, Virtual, 4–8 May 2020. [CrossRef]
10. Müller, M.; Kašpar, M.; Valeriánová, A.; Crhová, L.; Holtanová, E.; Gvoždíková, B. Novel indices for the comparison of precipitation extremes and floods: An example from the Czech territory. *Hydrol. Earth Syst. Sci.* **2015**, *19*, 4641–4652. [CrossRef]
11. Fetter, C.W. *Applied Hydrogeology*, 4th ed.; Prentice Hall, Inc.: Upper Saddle River, NJ, USA, 2001; 598p.
12. Directive. Directive 2006/118/EC of the European Parliament and of the Council. Directive on the protection of groundwater against pollution and deterioration. *Off. J. Eur. Communities* **2006**, *372*, 13.
13. Joseph, N.; Preetha, P.P.; Narasimhan, B. Assessment of environmental flow requirements using a coupled surface water-groundwater model and a flow health tool: A case study of Son River in the Ganga Basin. *Ecol. Indic.* **2020**, *121*, 107110. [CrossRef]
14. Čubanová, L.; Šoltész, A.; Bednárová, E.; Baroková, D.; Orfanus, M. Complex Proposal of Flood Protection Measures for Small Municipalities in the Area of Small Carpathians. In Proceedings of the 5th World Multidisciplinary Civil Engineering-Architecture-Urban Planning Symposium (WMCAUS), Prague, Czech Republic, 15–19 June 2020. [CrossRef]
15. Bear, J.; Verruijt, A. *Modeling Groundwater Flow and Pollution*; Springer: Dordrecht, Netherlands, 1992.
16. Peralta, R.C. *Groundwater Optimization Handbook: Flow, Contaminant Transport, and Conjunctive Management*; CRC Press: Roca Baton, FL, USA, 2012.
17. Thomas, A.; Eldho, T.I.; Rastogi, A.K.; Majumder, P. A comparative study in aquifer parameter estimation using MFree point collocation method with evolutionary algorithms. *J. Hydroinform.* **2019**, *21*, 455–473. [CrossRef]
18. Ghafoori, Y.; Vidmar, A.; Riha, J.; Kryzanowski, A. A Review of Measurement Calibration and Interpretation for Seepage Monitoring by Optical Fiber Distributed Temperature Sensors. *J. Sens.* **2020**, *20*, 5696. [CrossRef]
19. Ackerer, P.; Carrera, J.; Delay, F. Identification of aquifer heterogeneity through inverse methods. In *Special Issue: Geo-Hydrological Data & Models*; Institute de France, Académie des Sciences: Paris, France, 2022. [CrossRef]
20. Swathi, B.; Eldho, T.I. Aquifer parameter and zonation structure estimation using meshless local Petrov–Galerkin method and particle swarm optimization. *J. Hydroinform.* **2018**, *20*, 457–467. [CrossRef]
21. Koltsida, E.; Kallioras, A. Groundwater flow simulation through the application of the FREEWAT modeling platform. IWA Publishing. *J. Hydroinform.* **2019**, *21*, 812–833. [CrossRef]
22. Eryiğit, M. Estimation of parameters in groundwater modelling by modified Clonalg. *J. Hydroinform.* **2021**, *23*, 298–306. [CrossRef]
23. Evans, S.W.; Jones, N.L.; Williams, G.P.; Ames, D.P.; Nelson, E.J. Groundwater Level Mapping Tool: An open source web application for assessing groundwater sustainability. *Environ. Model. Softw.* **2020**, *131*, 104782. [CrossRef]
24. Hoffmann, J.; Sander, P. Remote sensing and GIS in hydrogeology. *Hydrogeol. J.* **2007**, *15*, 1–3. [CrossRef]
25. Senthilkumar, M.; Gnanasundar, D.; Arumugam, R. Identifying groundwater recharge zones using remote sensing & GIS techniques in Amaravathi aquifer system, Tamil Nadu, South India. *Sustain. Environ. Res.* **2019**, *29*, 15. [CrossRef]

26. Oyedele, A.A. Use of remote sensing and GIS techniques for groundwater exploration in the basement complex terrain of Ado-Ekiti, SW Nigeria. *Appl. Water Sci.* **2019**, *9*, 51. [CrossRef]
27. Lee, S.; Hyun, Y.; Lee, S.; Lee, M.-J. Groundwater potential mapping using remote sensing and GIS-based machine learning techniques. *Remote Sens.* **2020**, *12*, 1200. [CrossRef]
28. Al-Bahrani, H.; Al-Rammahi, A.; Al-Mamoori, S.; Almaliki, L.; Al-Ansari, N. Groundwater detection and classification using remote sensing and GIS in Najaf, Iraq. *Groundw. Sustain. Dev.* **2022**, *19*, 100838. [CrossRef]
29. Swain, N.R.; Christensen, S.D.; Snow, A.D.; Dolder, H.; Espinoza-Dávalos, G.; Goharian, E.; Jones, N.L.; Nelson, E.J.; Ames, D.P.; Burian, S.J. A new open source platform for lowering the barrier for environmental web app development. *Environ. Model. Softw.* **2016**, *85*, 11–26. [CrossRef]
30. Sege, J.; Ghanem, M.; Ahmad, W.; Bader, H.; Rubin, Y. Distributed data collection and web-based integration for more efficient and informative groundwater pollution risk assessment. *Environ. Model. Softw.* **2018**, *100*, 278–290. [CrossRef]
31. Sit, M.; Langel, R.J.; Thompson, D.; Cwiertny, D.M.; Demir, I. Web-based data analytics framework for well forecasting and groundwater quality. *Sci. Total Environ.* **2020**, *761*, 144121. [CrossRef] [PubMed]
32. Jones, D.; Jones, N.; Greer, J.; Nelson, J. A cloud-based MODFLOW service for aquifer management decision support. *Comput. Geosci.* **2015**, *78*, 81–87. [CrossRef]
33. Glass, J.; Junghanns, R.; Schlick, R.; Stefan, C. The INOWAS platform: A web-based numerical groundwater modelling approach for groundwater management applications. *Environ. Model. Softw.* **2022**, *155*, 105452. [CrossRef]
34. Collins, S.L.; Christelis, V.; Jackson, C.R.; Mansour, M.M.; Macdonald, D.M.J.; Barkwith, A.K.A.P. Towards integrated flood inundation modelling in groundwater-dominated catchments. *J. Hydrol.* **2020**, *591*, 125755. [CrossRef]
35. Merchán-Rivera, P.; Geist, A.; Disse, M.; Huang, J.; Chiogna, G. A Bayesian framework to assess and create risk maps of groundwater flooding. *J. Hydrol.* **2022**, *610*, 127797. [CrossRef]
36. Julínek, T.; Duchan, D.; Říha, J. Mapping of uplift hazard due to rising groundwater level during floods. *J. Flood Risk Manag.* **2020**, *13*, e12601. [CrossRef]
37. Kumar, R.; Yazdan, M.S. Evaluating Preventive Measures for Flooding from Groundwater: A Case Study. *J. Multidiscip. Sci. J.* **2023**, *6*, 1–16. [CrossRef]
38. Yu, X.; Moraetis, D.; Nikolaidisc, N.P.; Lid, B.; Duffye, C.; Liu, B. A coupled surface-subsurface hydrologic model to assess groundwater flood risk spatially and temporally. *Environ. Model. Softw.* **2019**, *114*, 129–139. [CrossRef]
39. Joo, J.; Tian, Y. Impact of Stream-Groundwater Interactions on Peak Streamflow in the Floods. *Hydrology* **2021**, *8*, 141. [CrossRef]
40. Peña, F.; Nardi, F.; Melesse, A.; Obeysekera, J.; Castelli, F.; Price, R.M.; Crowl, T.; Gonzalez-Ramirez, N. Compound flood modeling framework for surface–subsurface water interactions. *J. Nat. Hazards Earth Syst. Sci.* **2022**, *22*, 775–793. [CrossRef]
41. Ferraz, G.; Krámer, T. Surface Water–Groundwater Interactions and Bank Storage during Flooding: A Review. *Period. Polytech. Civ. Eng.* **2022**, *66*, 149–163. [CrossRef]
42. Wei, S.; Zheng, Y.; Liang, X.; Xu, P.; Tian, Y.; Frame, J.M.; Zhang, Y. A distributed domain model coupling open channel flow and groundwater flow to quantify the impact of lateral hydrologic exchange on hydrograph. *J. Hydrol.* **2022**, *611*, 128010. [CrossRef]
43. Naughton, O.; McCormack, T.; Gill, L.; Johnston, P. Groundwater flood hazards and mechanisms in lowland karst terrains. In *Advances in Karst Research: Theory, Fieldwork and Applications*; Parise, M., Gabrovsek, F., Kaufmann, G., Ravbar, N., Eds.; Geological Society, London, Special Publications: London, UK, 2018; Volume 466, pp. 397–410.
44. Fell, R.; Fry, J.J. The state of the art of assessing the likelihood of internal erosion of embankment dams, water retaining structures and their foundations. In *Internal Erosion of Dams and their Foundations*; Taylor and Francis: London, UK, 2007; pp. 1–23.
45. IPCC. Managing the Risks of Extreme Events and Disasters to Advance Climate Change Adaptation: Special Report of the Intergovernmental Panel on Climate Change. 2012. Available online: https://www.ipcc.ch/pdf/special-reports/srex/SREX_Full_Report.pdf (accessed on 20 January 2023).
46. Pinder, G.F.; Gray, W.G. *Finite Element Simulation in Surface and Subsurface Hydrology*; Academic Press: New York, NY, USA; San Francisco, CA, USA; London, UK, 1977; 295p.
47. Galavi, V. *Groundwater Flow, Fully Coupled Flow Deformation and Undrained Analyses in PLAXIS 2D and 3D*; PLAXIS BV. Research Department: Delft, NL, USA, 2010; 285p.
48. GMS. Groundwater Modeling System GMS 10.7. Aquaveo, Provo, USA. 2021. Available online: https://www.aquaveo.com/software/gms-groundwater-modeling-system-introduction (accessed on 2 February 2023).
49. ANSYS. Engineering Simulation Software. 2023. Available online: https://www.ansys.com/ (accessed on 2 February 2023).
50. Hálek, V.; Švec, J. *Groundwater Hydraulics*; Academia: Prague, Czech Republic, 1979; 620p.
51. Moghadam, Z.; Jahanshahi, R.; Asadi, N.; Behzadifar, V. Factors affecting on the groundwater uplift in the Mashhad city, Iran. *Iran. Water Res. J.* **2019**, *14*, 13.
52. *EN1997-1:2004*; Eurocode 7: Geotechnical Design. European Committee for Standardisation: Brussels, Belgium, 2004; 105p.
53. De Caro, M.; Crosta, G.B.; Previati, A. Modelling the interference of underground structures with groundwater flow and remedial solutions in Milan. *J. Eng. Geol.* **2020**, *272*, 105652. [CrossRef]
54. Frick, M.; Scheck-Wenderoth, M.; Schneider, M.; Cacace, M. Surface to Groundwater Interactions beneath the City of Berlin: Results from 3D Models. *J. Geofluids* **2019**, *Volume 2019*, 4129016. [CrossRef]
55. Jandora, J.; Říha, J. Groundwater flow modelling of the flood protection measures in Prague-Troja. *Water Manag.* **2008**, *58*, 68–73.

56. Dagan, G. An overview of stochastic modeling of groundwater flow and transport: From theory to applications. *Eos Trans. Am. Geophys. Union* **2002**, *83*, 621–625. [CrossRef]
57. Rwanga, S.; Ndambuki, J. Solving groundwater problems fraught with uncertain recharge: An application to Central Limpopo, South Africa. *Groundw. Sustain. Dev.* **2020**, *10*, 100305. [CrossRef]